Contract NAS8-30246

STUDY OF MULTIPLE HOLOGRAM RECORDING IN LITHIUM NIOBATE

T. K. Gaylord and W.R. Callen
School of Electrical Engineering
Georgia Institute of Technology
Atlanta, Georgia 30332

October 1974

FINAL REPORT FOR PERIOD 1 OCTOBER 1973 – 31 OCTOBER 1974

1974

Performed for

National Aeronautics and Space Administration
George C. Marshall Space Flight Center
Marshall Space Flight Center, Alabama 35812

SCHOOL OF ELECTRICAL ENGINEERING
Georgia Institute of Technology
Atlanta, Georgia 30332

FINAL REPORT

PROJECT NO. E-21-633

STUDY OF MULTIPLE HOLOGRAM RECORDING IN LITHIUM NIOBATE

by

T. K. Gaylord and W. R. Callen

RESEARCH CONTRACT NAS8-30246

1 October 1973 to 31 October 1974

Performed for

NATIONAL AERONAUTICS AND SPACE ADMINISTRATION
George C. Marshall Space Flight Center
Marshall Space Flight Center, Alabama 35812

ABSTRACT

The results of detailed experimental and theoretical considerations relating to multiple hologram recording in lithium niobate is reported. The following problem areas are identified and discussed: 1) the angular selectivity of the stored holograms, 2) interference effects due to the crystal surfaces, 3) beam divergence effects, 4) material recording sensitivity, and 5) scattered light from material inhomogeneities.

TABLE OF CONTENTS

LIST OF FIGURES

I. INTRODUCTION

A program to study high capacity recording in electro-optic crystals was undertaken. This study focused on the problems associated with very high capacity storage (through multiple hologram superposition) and the use of lithium niobate as the recording medium.

A number of important problem areas were identified and studied. These included: 1) the angular selectivity of the stored holograms, 2) interference effects due to the crystal surfaces, 3) beam divergence effects, 4) material recording sensitivity, and 5) scattered light from material inhomogeneities.

Single hologram and multiple hologram recording experiments were performed on a vibration isolation table with an argon laser using the experimental configuration shown in Fig. 1. Holograms were analyzed experimentally by reading them with laser light of 488.0nm, 514.5nm, and 632.8nm wavelength.

To properly interpret the above experimental results, a number of analytical studies were initiated to provide predictions of the read-out parameters of the volume holograms.

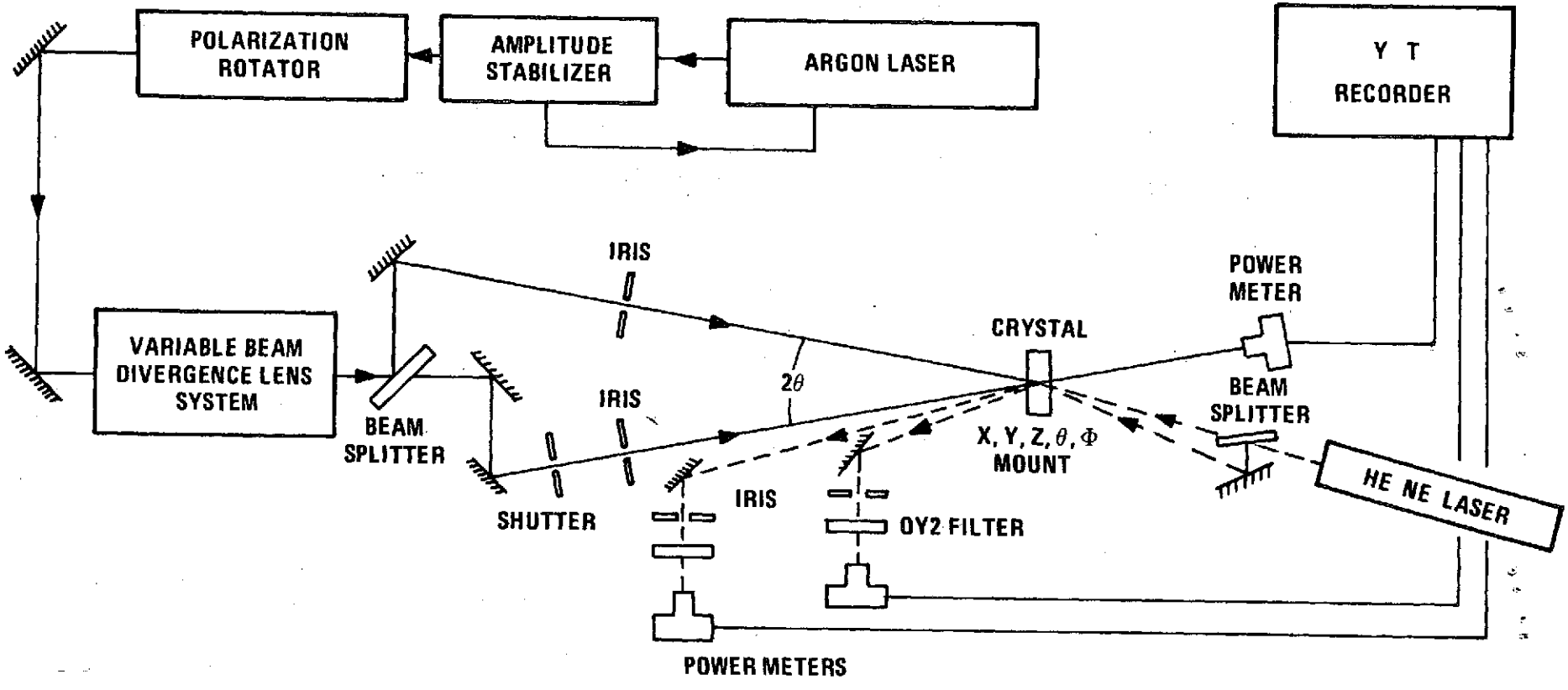

FIGURE 1. EXPERIMENTAL CONFIGURATION FOR MEASURING THE OPTICAL HOLOGRAPHIC STORAGE PROPERTIES OF FERROELECTRIC CRYSTALS.

II. ANGULAR SELECTIVITY

Because of the three-dimensional nature of the crystal, holograms recorded in lithium niobate are volume holograms. These holograms are produced directly (without processing) by the interference of laser beams of the appropriate wavelength intersecting in the crystal. The volume nature of this holographic storage is especially interesting since it indicates the possibility of very high capacity information storage.

Volume (thick) holograms exhibit a number of properties in addition to those possessed by two-dimensional (thin) holograms. Among these properties is angular selectivity—the need for the reference beam to illuminate the hologram at a precise angle in order to achieve reconstruction. Illumination outside of this angular corridor produces a rapidly decreasing intensity of the reconstructed data. To perform these diagnostic experiments plane wave holograms (caused by the interference of two plane waves) were used. Even though this is a special case, a general hologram may be constructed by the superposition of an infinite number of plane wave holograms. Reconstruction of a volume hologram [1] is possible (with half maximum diffracted power or greater) only over the range of wavelengths given by

$$\frac{\Delta\lambda}{\lambda} \simeq \cot\ \theta\ \frac{L}{t} \tag{1}$$

and only over the range of angles given by

$$\Delta\theta \simeq A(\eta_o)n(\lambda,P)\ \frac{L}{t}\ , \tag{2}$$

where $\Delta\lambda$ and $\Delta\theta$ are centered about the writing wavelength λ, and the writing angle, θ. The thickness of the hologram is given by t, L is the fringe

spacing of the fundamental grating ($L = \lambda/2\sin\theta$), $n(\lambda,P)$ is the appropriate index of refraction for the probing beam wavelength and polarization, and $A(\eta_b)$ is the angular selectivity coefficient (approximately equal to unity). These types of properties are in actuality just manifestations of the increased storage capacity of the volume storage medium.

The experimental configuration shown in Figure 1 was used to measure the angular selectivity and compare it with the theoretical value. Thicknesses from 1mm to 5mm were tested. Both iron-doped and nominally pure crystals of lithium niobate were used. The half-power angular widths were found to be in agreement with theoretically predicted values. These results show that the theoretical angular packing density of multiple holograms is achievable! This important finding was reported in Appl. Phys. Letters [2]. This publication gives experimental details as well as results and is reproduced here for completeness.

Additional experimental results have been obtained since Ref. 2 was published. These show a much more detailed comparison of theory and experiment for a broader range of reading angles. These data are shown in Figs. 2 and 3.

ANGULAR SELECTIVITY OF LITHIUM NIOBATE VOLUME HOLOGRAMS

T. K. GAYLORD
School of Electrical Engineering, Georgia Inst. of Technology Atlanta, Georgia

F K TITTEL
Electric Engineering Department Rice Univ. Houston Texas

PAPER INTENTIONALLY OMITTED

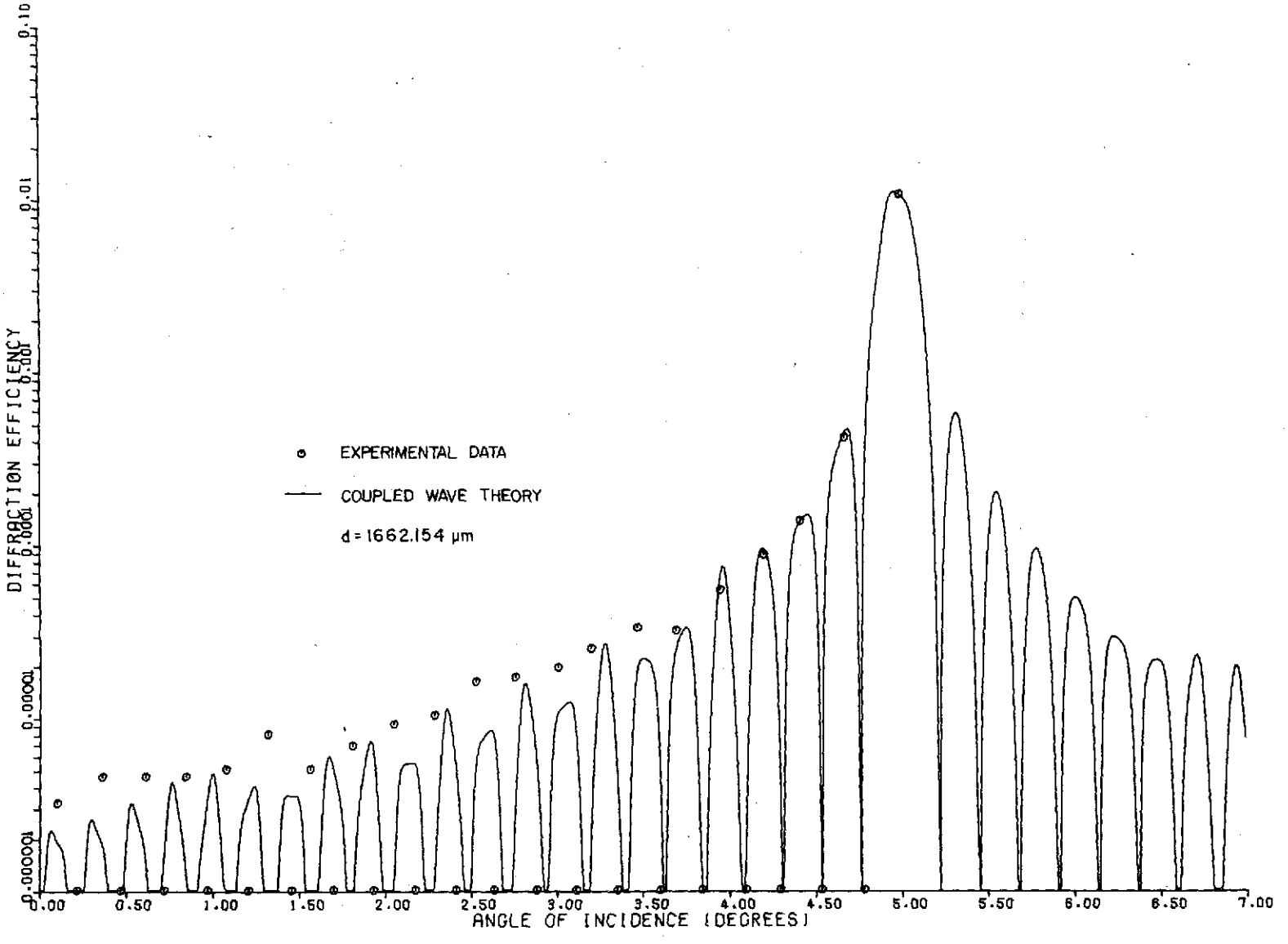

FIGURE 2. A COMPARISON OF ANGULAR SELECTIVITY EXPERIMENTAL DATA WITH RESULTS FROM THE COUPLED WAVE THEORY. The particular thickness chosen, d, yields the best fit close to the Bragg angle.

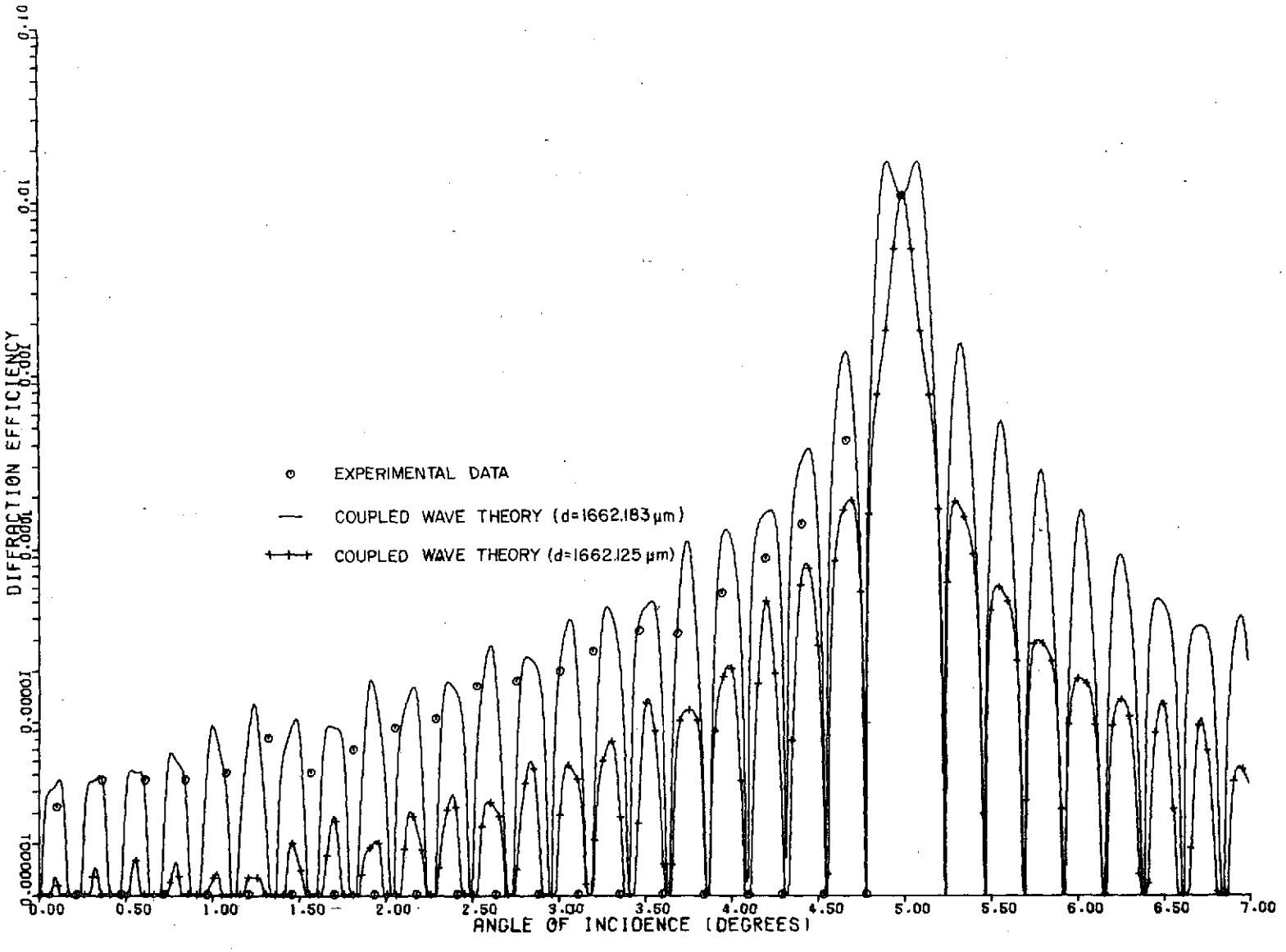

FIGURE 3. AMPLITUDE RANGE OF THEORETICAL ANGULAR SELECTIVITY DUE TO MINUTE THICKNESS VARIATIONS. The thickness used in producing the plain curve is that needed to obtain a minimum value of the transmittance factor on the Bragg angle ($\tau = 0.3$). The crossed curve corresponds to maximum transmittance ($\tau = 1.8$). The experimental data is seen to occur within these extremes.

III. SURFACE INTERFERENCE EFFECTS

Many analyses of hologram reconstruction do not account for boundary (surface) reflections. The diffraction efficiency results may be corrected to include boundary reflections by multiplying by a transmittance factor. This factor, τ, is developed by us in Ref. 3, a copy of which is included in this report. This factor is the same as the transmittance factor derived by Kogelnik and given as Eq. (8) in Ref. 4, but with νd in that equation replaced by the argument of the sine function in Eq. (27) in our paper [3].

From these results, we find that boundary reflections produced by the surfaces can considerably change the diffraction efficiency. The change can be an increase or a decrease depending on whether the transmittance factor is greater or less than unity. This effect has been studied by Cohen and Gordon [5]. For the grating parameters used here, τ is typically in the range 0.70 to 1.20. In practice, the boundary reflections can be eliminated by antireflection coatings on the surfaces of the gratings.

Calculated results showing the thickness dependence of τ for lithium niobate are shown in Fig. 4. The effect of τ as a function of reading angle is shown in Fig. 5.

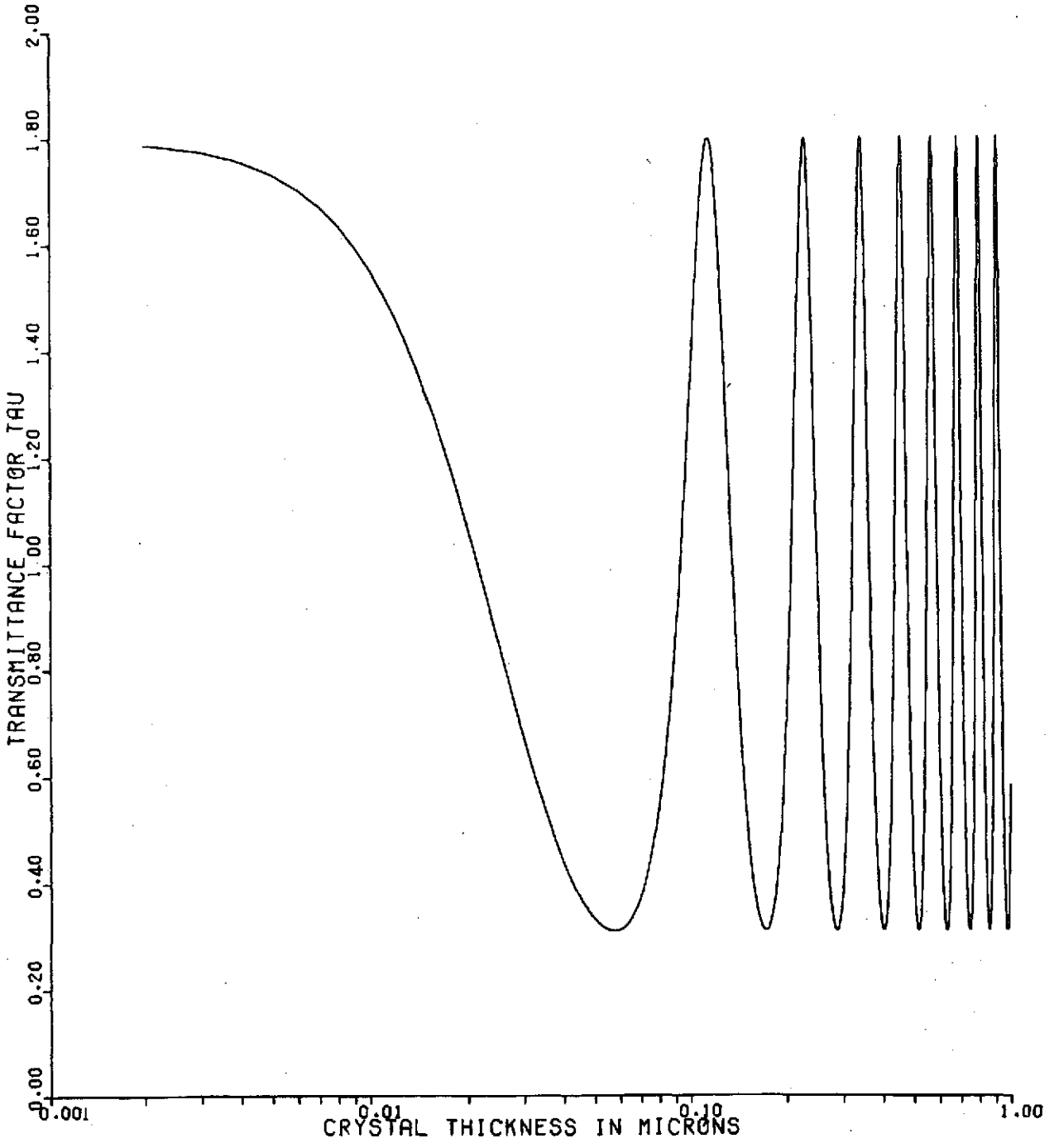

FIGURE 4. TRANSMITTANCE FACTOR, τ, AS A FUNCTION OF CRYSTAL THICKNESS.

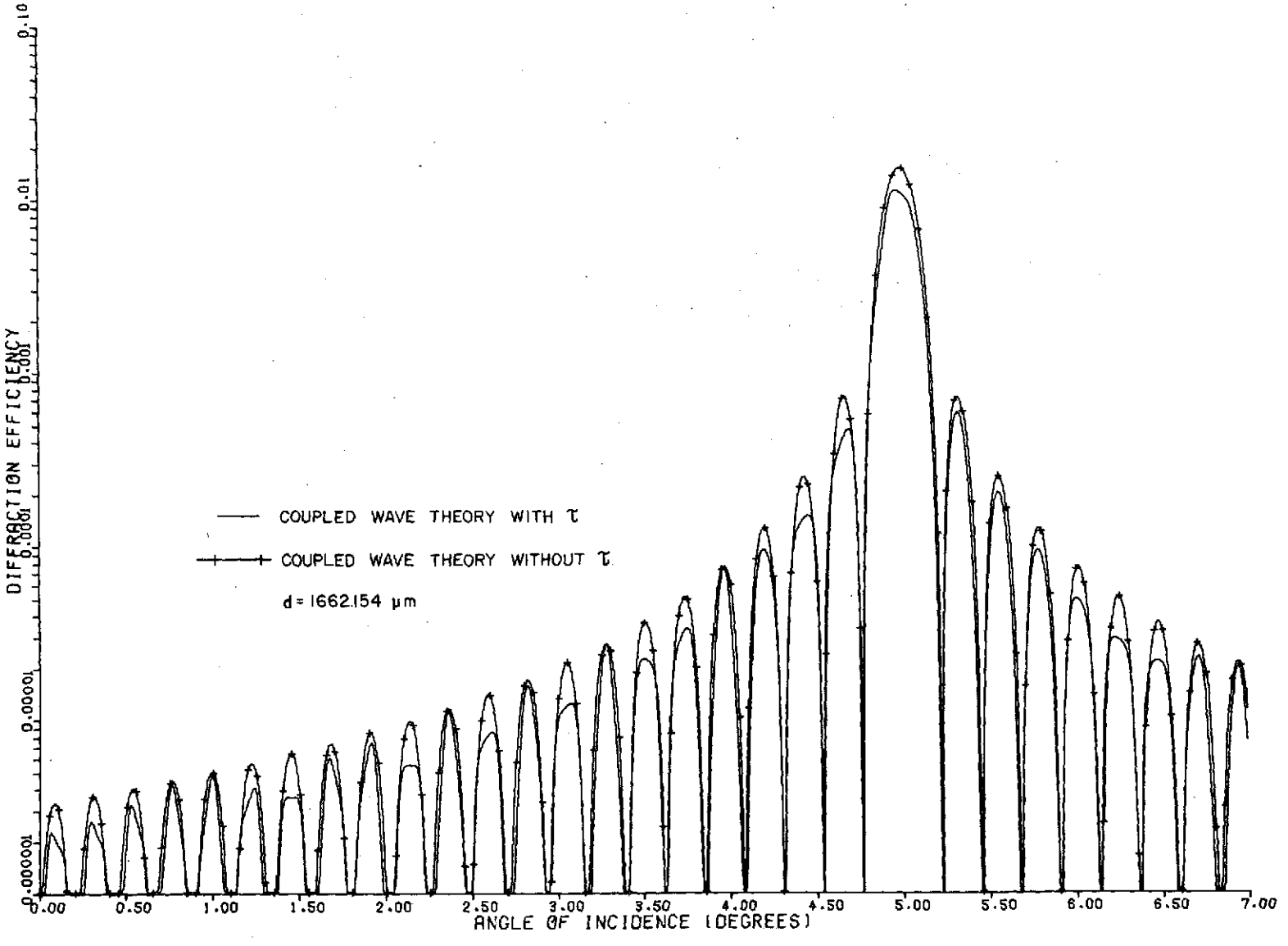

FIGURE 5. EFFECT OF THE TRANSMITTANCE FACTOR ON ANGULAR SELECTIVITY.

IV. BEAM DIVERGENCE EFFECTS

The effect of writing beam divergence was studied. First, a hologram was written with a frequency doubled Nd:YAG laser (λ = 530nm) with a beam divergence of 0.143^{o}. Second, a hologram was written with an argon laser (λ = 514.5nm) with a beam divergence of 0.035^{o}. The angular selectivities of these holograms were then measured with a He-Ne laser. The half-power angular width in both cases was found to be within 10% of the theoretical value derived in our paper [2]. Thus, it was concluded that writing beam divergence has little effect on the final read-out process.

V. RECORDING SENSITIVITY

Recording materials must possess a number of important characteristics to achieve the high storage capacities that have been predicted for optical memories. These requirements on the optical recording material include: 1. High sensitivity—It is desirable that only a small amount of optical energy per unit area be needed to record the hologram of a data page. Table 3 in Ref. 6 (reproduced later in this report) lists the necessary writing energy densities for a number of recording materials. For a practical system an energy density of about 1 millijoule/cm^2 or less will be needed. 2. Large diffraction efficiency—Diffraction efficiency is the fraction of the reading light (reference beam) that is diffracted into the reconstructed data beam. It must be possible to record a single hologram with a large diffraction efficiency, so that in practice many holograms may be recorded at a single location, each with an equal share of the total maximum diffraction efficiency. Therefore, it is desirable to have the maximum diffraction efficiency as close to 100% as possible. 3. Erasable and rewritable—For a rapid cycle read-write-erase memory system, it must be possible to continuously alter the stored data in the memory without encountering any degradation in the material characteristics. 4. Long lifetime of stored information—Stored data should persist for long periods of time before having to be refreshed. Ideally, storage should be permanent. 5. Non-volatile storage—Data should remain recorded in the memory in the absence of system power. 6. Nondestructive readout—It should be possible to perform an essentially unlimited number of read operations without degrading or altering the stored data. 7. Three dimensional storage—To achieve very high capacity storage, the information should be stored in thick (volume) holograms. Together with the requirement of high diffraction efficiency, this means that the hologram

should be a thick phase (nonabsorbing) hologram. 8. High resolution— The storage material obviously must be capable of recording the very fine (wavelength size) variations of the interference pattern produced by the intersection of the object and reference beams.

Considering all of the above material requirements, the photorefractive materials (optically induced changes in index of refraction) appear to be especially promising. These materials, often ferroelectric crystals such as lithium niobate and strontium barium niobate (SBN), have been considerably developed and improved. For example, in the first use of lithium niobate as a recording material in 1968 a writing energy density of approximately 100 joules/cm^2 was required [7]. Less than six years later, doped versions of lithium niobate have now been shown in this work to exhibit writing energy densities of 2 millijoules/cm^2! We have announced this improvement in sensitivity of almost 5 orders of magnitude in Applied Physics Letters [8]. This article is reproduced here for completeness. Fig. 6 depicts this recent jump in sensitivity with respect to other potential recording materials. In addition, recent work by von der Linde et al. [9] indicates that even higher sensitivities are possible in lithium niobate!

VOLUME HOLOGRAPHIC RECORDING AND STORAGE IN Fe-DOPED $LiNbO_3$ USING OPTICAL PULSES

PRADEEP SHAH, T A RABSON AND F K TITTEL
Department of Electric Engineering Rice Univ. Houston Texas

T K GAYLORD

PAPER INTENTIONALLY OMITTED

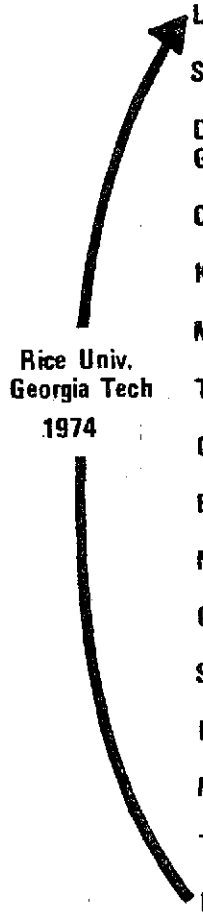

Material	Type of Material	Writing Energy Density (joules/cm^2)
$Bi_{12}Si\ O_{20}$	Ferroelectric–Photoconductive	1×10^{-5}
Malachite Green: Sucrose Benzoate	Thermoplastic	2×10^{-5}
Agfa 8E70	Photographic	2×10^{-5}
Kodak 649F	Photographic	7×10^{-5}
$Bi_4Ti_3O_{12}$–ZnSe	Ferroelectric–Photoconductive	1×10^{-3}
$LiNbO_3$:Fe	Photorefractive	2×10^{-3}
$Sr_{0.75}Ba_{0.25}Nb_2O_6$	Photorefractive	6×10^{-3}
Dichromated Gelatin	Photochemical	9×10^{-3}
$Ca\ F_2$: Ce	Photochromic	1×10^{-2}
KCL:Na	Photochromic	1×10^{-2}
Mn Bi	Magnetooptic	3×10^{-2}
$Te_{88}Ge_7As_5$	Amorphous Semiconductor	5×10^{-2}
Gd I G	Magnetooptic	9×10^{-2}
Eu O	Magnetooptic	9×10^{-2}
Na F	Photochromic	9×10^{-2}
Co–P–Ni–Fe	Magnetooptic	1×10^{-1}
$SrTiO_3$:Ni:Mo	Photochromic	2×10^{-1}
Ba Ti O_3	Photorefractive	2×10^{-1}
Mn Al Ge	Magnetooptic	3×10^{-1}
$Te_{81}Ge_{15}Sb_2S_2$	Amorphous Semiconductor	5×10^{-1}
$LiNbO_3$:Fe	Photorefractive	8×10^{-1}
KBr	Photochromic	1
$Cu_2Hg\ I_4$	Thermoplastic	3
$BaNaNb_5O_{15}$	Photorefractive	5
$Bi_4Ti_3O_{12}$	Photorefractive	10
$Sr_{0.75}Ba_{0.25}Nb_2O_6$	Photorefractive	14
$LiNbO_3$	Photorefractive	100

FIGURE 6. REQUIRED WRITING ENERGY DENSITY FOR VARIOUS OPTICAL RECORDING MATERIALS.

VI. SCATTERED LIGHT EFFECTS

Scattered light during hologram reconstruction has been recognized as a problem for high capacity storage in lithium niobate [10].

We have reported [11] the presence of cones of diffracted light upon illumination of previously laser-exposed crystals of lithium niobate. These diffraction cones are shown to result from the internally recorded interference pattern (hologram) resulting from the interference of the original incident laser beam with light scattered from material inhomogeneities. Diffraction cones are observed in iron-doped lithium niobate crystals that were exposed to a single laser beam and in crystals that were exposed to two superposed laser beams (i.e., during conventional holographic recording). In the two beam case, the diffraction cones are present in addition to the first order diffracted beam when the conventional two beam thick hologram is reconstructed. The diffracted cones produce the impression of scattered light during hologram reconstruction, an effect that has previously been reported in transition metal doped lithium niobate [10].

The diffraction cones, which have their apex in the exposed region of the crystal, are observed as rings (referred to as "scattering" rings, or diffraction rings) when a screen or a piece of film intersects the cone of light. Figure 1 in Reference 11 shows two typical diffraction ring patterns. For the single beam case, the observed results in lithium niobate are effectively the same as the experimental observations of Moran and Kaminow [12] for polymethyl methacrylate (PMMA), which had been exposed to ultraviolet laser light.

The presence of diffracted cones of light represents a possible limitation of heavily iron doped lithium niobate for data storage applications

because optical power is lost into the scattering induced diffraction cones that could otherwise be used to increase the diffraction efficiency and thus the total bit capacity of the two beam grating hologram. However, it has already been shown by Phillips, Amodei, and Staebler [10] that the "scattered" light may be erased 1) by illumination with uniform incoherent light or 2) by writing additional superposed holograms at new angles. In the latter case, "scattered" light from the previous holograms tends to be erased.

Our Ref. 11 is reproduced here for completeness.

LASER SCATTERING INDUCED HOLOGRAMS IN LITHIUM NIOBATE

R MAGNUSSON AND T K GAYLORD

School of Electric Engineering Georgia Inst. of Technology, Atlanta, Georgia

PAPER INTENTIONALLY OMITTED

VII. MULTIPLE HOLOGRAM STORAGE

In the last four sections, problems associated with multiple hologram storage have been discussed. The experimental results presented have been obtained using the basic experimental configuration shown in Fig. 1. Basic diagnostic experiments were performed by storing both single holograms and by storing multiple holograms [13] at a single location. The theoretical storage density of two dimensional (thin) holograms is 4×10^8 bits/cm^2 (one bit per square area one wavelength on a side) whereas in three dimensional volume (thick) holograms the theoretical storage density is 8×10^{12} bits/cm^3 (one bit per cube volume wavelength on a side) [14]. Obviously for truly high capacity storage, thick holograms (such as in optical crystals) need to be used instead of thin holograms (such as in photographic emulsions or metal films). Holographic memory systems have been described that utilize three-dimensional storage [15]. These systems superpose many holograms at a single location inside the thick recording medium by using a different reference beam angle for each hologram. The superposition of multiple holograms at a single volume location introduces the additional problem of writing new holograms in that volume without affecting those already there. When lithium niobate is used as the three dimensional storage material, this problem may be solved by the application of an external electric field [16], [17]. This greatly increases the sensitivity for writing while the sensitivity for erasure remains unchanged at a much lower value. Thus, as a new hologram is written, the other holograms at that location are only slightly erased. Work is presently underway in our laboratory to duplicate these electric field effects.

VIII. RECORDED HOLOGRAM ANALYSIS

A method for analyzing the diffraction efficiency of thick, lossless transmission holograms in lithium niobate was developed. In lithium niobate and similar ferroelectrics, the literature assumes the induced changes in index of refraction are sinusoidal in nature, like the two beam plane wave interference pattern. The diffraction efficiency can be predicted for the sinusoidal case [1]. In actual fact, the index of refraction variation is probably not sinusoidal due to the obviously nonlinear writing characteristic (diffraction efficiency versus exposure), which is experimentally observed.

We have developed [3] a method for calculating arbitrary-order diffraction efficiencies of thick, lossless transmission gratings with arbitrary periodic grating shapes. For illustration, numerical values of the diffraction efficiencies at the first three Bragg angles were calculated for sinusoidal, square wave, triangular, and sawtooth gratings. The complete details of this method are expounded in Ref. 3, which is duplicated in this report. Also a comparison of our method to an extension of the Burckhardt matrix method [18] is presented in Fig. 7. Our method was determined to be 20 times faster on the computer!

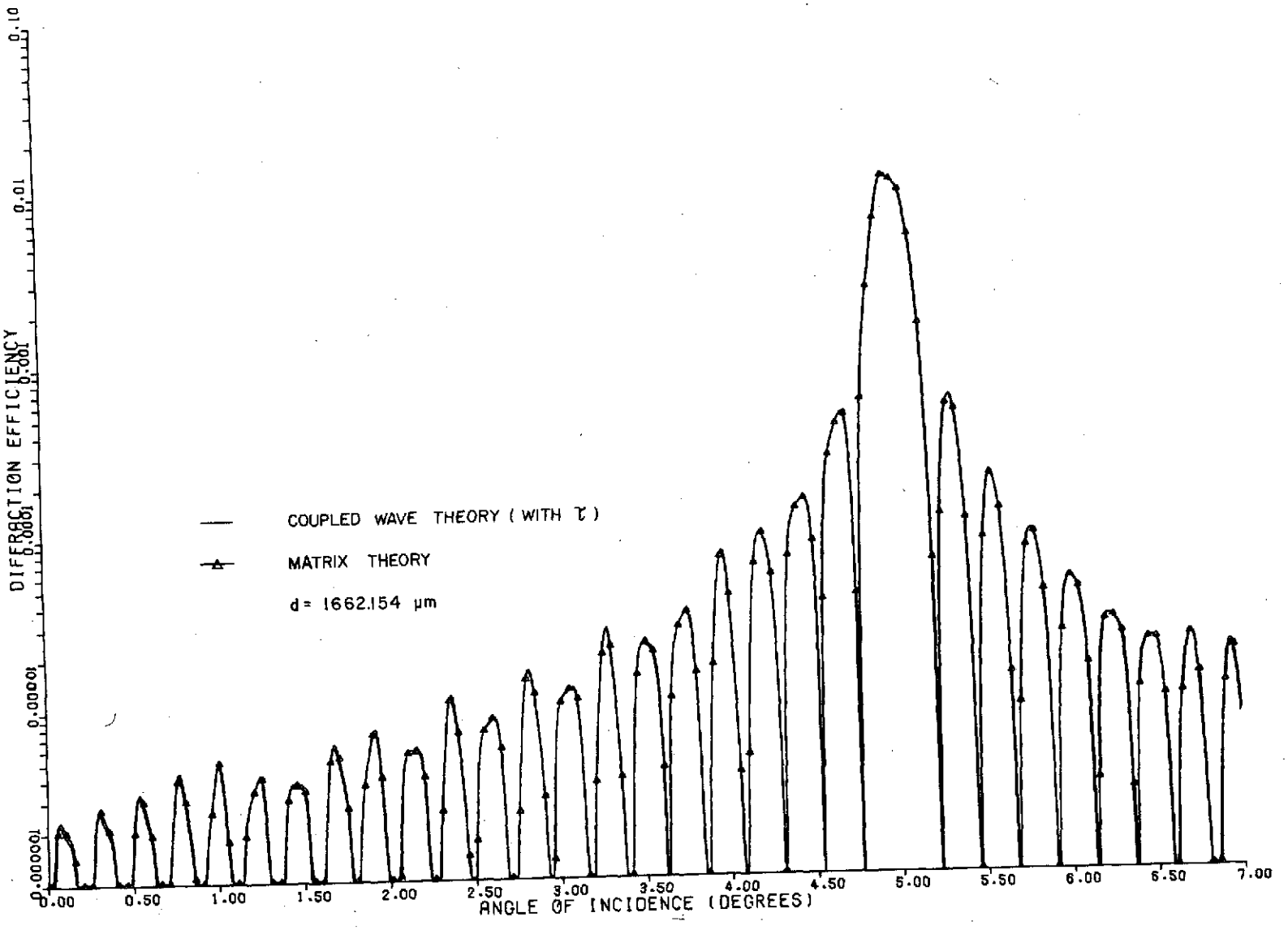

FIGURE 7. COMPARISON OF COUPLED-WAVE AND MATRIX THEORIES. The plot actually consists of two curves, but the difference is not discernible.

Journal of the Optical Society of America, vol. 65, no. 1, January 1975.

Calculation of arbitrary-order diffraction efficiencies of thick gratings with arbitrary grating shape*

S. F. Su and T. K. Gaylord

School of Electrical Engineering, Georgia Institute of Technology, Atlanta, Georgia 30332

(Received 18 July 1974, revision received September 1974)

A method for calculating arbitrary-order diffraction efficiencies of thick, lossless transmission gratings with arbitrary periodic grating shapes has been developed. This represents an extension of previous work to nonsinusoidal gratings and to higher-order Bragg angles. A Fourier-series representation of the grating is employed, along with a coupled-mode theory of diffraction. For illustration, numerical values of the diffraction efficiencies at the first three Bragg angles are calculated for sinusoidal, square-wave, triangular, and saw-tooth gratings. Numerical results for the same grating shapes with the same parameters are also calculated for comparison, by extending Burckhardt's numerical method for analyzing thick sinusoidal gratings. The comparison shows that the coupled-mode theory provides results with relative computational ease and results that are in agreement with calculations obtained by extending the more-rigorous Burckhardt theory to nonsinusoidal grating shapes and to higher-order Bragg angles.

Index Headings: Gratings, Diffraction.

It is well known that thick dielectric diffraction gratings differ from thin gratings in a number of important ways. Among these are the capability of high diffraction efficiency,[1] wavelength selectivity,[1] angular selectivity,[1] and reduced noise.[2] These give rise to the use of thick gratings as highly efficient diffraction gratings, narrow-band spectral filters,[3] thick-grating optical components, such as lenses,[4] and imaging systems capable of spectral resolution of extended objects.[2] In the field of integrated optics, thick gratings may be used as diffraction gratings for surface guiding of waves,[5] for thin-film distributed-feedback lasers,[6] for frequency-selective grating reflectors in thin-film lasers,[7] for grating couplers for launching single-mode light waves into thin-film waveguides,[8,9] and for electro-optic grating deflectors and modulators.[10]

In addition, thick (volume) holograms may be regarded as recordings of an infinite number of thick gratings. Thick holograms have attracted a great deal of interest by their use in high-capacity information storage,[11] in color holography,[12] and in white-light reconstruction of holograms.[13]

The diffraction of a plane wave by a thick sinusoidal grating at or near Bragg incidence has been considered by Burckhardt[14] and by Kogelnik.[1] Burckhardt has treated this case by solving the exact electromagnetic boundary-value problem and has obtained numerical results with a digital computer to determine the eigenvalues of a matrix and to solve the resulting set of linear algebraic equations. Kogelnik has obtained a closed-form expression for the diffraction efficiency at the first-order Bragg angle, by employing a coupled-wave theory. Coupled-wave theories also have been used successfully in the treatment of light diffraction by acoustic waves.[15,16] Recently, Chu and Tamir[17] treated this problem by using a guided-wave

technique. They assumed sinusoidal modulation of the relative permittivity by the sound wave. Their treatment was based on a rigorous modal approach, utilizing the interrelationships between the characteristic mode and the coupled-mode representations. With their method, not only the diffraction efficiency at the first order but also that of any higher order can be obtained.

In this paper, Chu and Tamir's approach is extended to examine the first- and higher-order diffraction efficiencies of thick, arbitrary-shape gratings. Because of the periodicity of the grating, a Fourier-series representation of the grating is employed. The gratings are assumed to be lossless. The reflections at surfaces of the gratings are at first neglected in the derivation, because, in practice, these can be eliminated by antireflection coatings. When surface and internal reflections are present, the results are corrected by a multiplicative transmittance factor.[18] For illustration, numerical values of the diffraction efficiencies at the first three Bragg angles are calculated for sinusoidal, square-wave, triangular, and saw-tooth gratings. For comparison, numerical results for the same grating shapes with the same parameters are also calculated by extending Burckhardt's numerical method. The comparison shows that the results from these two methods are in close agreement and that the present method is computationally simpler and more efficient.

THEORETICAL ANALYSIS

The model for a thick periodic grating can be described by Fig. 1. The x axis is chosen in the plane of incidence and parallel to the surfaces of the medium, the z axis is perpendicular to the surfaces of the medium, and the y axis is perpendicular to the page. For convenience, the fringe planes of the grating are assumed to be perpendicular to the surfaces of the medium and to the plane of incidence. The grating vector $\bar{K}$ is, therefore, parallel to the x axis. Thus, for lossless periodic gratings, the fringes of the grating can be represented by a spatial modulation of the relative dielectric constant,

$$\epsilon_r(x) = \epsilon(x)/\epsilon_o = \epsilon_{ro} + \sum_{h=1}^{\infty} [\epsilon_{ch}\cos(hKx) + \epsilon_{sh}\sin(hKx)], \qquad (1)$$

where $K = 2\pi/L$, L is the period of the grating, ϵ_{ro} is the average value of ϵ_r, and ϵ_{ch} and ϵ_{sh} are the spatial modulations of ϵ_r, the subscripts c, s and h denoting the quantities connected with the cosine gratings, the sine gratings and the h th-harmonic grating, respectively. Corresponding to the distribution of the relative dielectric constant, the distribution of the refractive index of the medium is

$$n(x) = n_o + \sum_{h=1}^{\infty} [n_{ch}\cos(hKx) + n_{sh}\sin(hKx)], \qquad (2)$$

where n_o is the average refractive index of the medium, and n_{ch} and n_{sh} are the spatial modulations of n.

The electric field of the incident wave is assumed to be polarized perpendicular to the plane of incidence (H mode) and is of the form

$\exp[j(\eta_o x + \xi_o z - \omega_o t)]$. The wave propagation in the grating can be described by the scalar wave equation

$$[\nabla^2 + k^2 \epsilon_r(x)]\, E(x,z) = 0, \tag{3}$$

where $k = 2\pi/\lambda$, λ is the free-space wavelength of the incident plane wave, and $E(x,z)$ is the complex amplitude of the y component of the electric field, which is independent of y.

Eq. (3) has been solved by Burckhardt,[14] using separation of variables, an infinite-series solution for the x-dependent equation, and a matrix method to solve the eigenvalue problem associated with a truncated set of the resulting infinite system of equations. This approach has been used to obtain numerical results for sinusoidal gratings. Kaspar[19] has extended Burckhardt's method to find the diffraction efficiency for nonsinusoidal absorption gratings. He has pointed out that when the absorption is strong, the phase-grating contribution to the diffraction efficiency is very small.

Chu and Tamir[17] have shown that the field inside the grating can be described in terms of coupled modes if the modulations of the relative dielectric constant are very small. In general, in addition to the zeroth mode, many higher-order modes are excited, because of the presence of the grating. For an incident wave (zero-order mode) of wavelength λ, and at an angle θ_o, the fundamental grating will diffract this wave if the Bragg condition, $m\lambda = 2L \sin\theta_o$, is satisfied or nearly satisfied. For this particular wavelength and angle, the harmonic gratings may or may not produce diffraction, depending on whether or not their corresponding Bragg conditions are satisfied or nearly satisfied. These diffracted modes of the fundamental and the harmonic gratings propagate in the same direction.

The dimensionless quantities

$$q_{ch} = 2\left(\frac{L}{h\lambda}\right)^2 \epsilon_{ch}, \qquad h = 1, 2, 3, \ldots \tag{4}$$

$$q_{sh} = 2\left(\frac{L}{h\lambda}\right)^2 \epsilon_{sh}, \qquad h = 1, 2, 3, \ldots \tag{5}$$

are called the effective-modulation indices.[17,20] Because ϵ_{ch} and ϵ_{sh} would typically be 10^{-4} or smaller, q_{ch} and q_{sh} are small even if L is many times as large as λ. For example, if $\theta_o = 5^o$ and $\epsilon_{c1} = 10^{-4}$, then $q_{c1} = 0.0066$. When q is very small compared to unity, it can be shown[17,21] that two coupled-wave equations and therefore two modes are sufficient to describe the coupling effects when the incident angle is equal to or near the Bragg angle. Therefore, for an incident wave of wavelength λ and at an angle θ_o, the electric field inside the grating can be written as the sum of the fundamental mode and an arbitrary mode

$$\tilde{E}(x,z) = \tilde{S}_o(z) \exp(j\tilde{\eta}_o x) + \tilde{S}_m(z) \exp(j\tilde{\eta}_m x), \tag{6}$$

where $\tilde{\eta}_o$ and $\tilde{\eta}_m$ are the zeroth-mode and the m th-mode (with respect to the fundamental grating) transverse wave numbers, respectively. The continuity of the electric field at z = 0 and the Floquet theorem require that $\tilde{\eta}_o = \eta_o = k \sin\theta_o$ and $\tilde{\eta}_m = \eta_m = \eta_o - 2m\pi/L$. The tilde ~ will henceforth be used to denote the quantities in the dielectric medium when the gratings are present. The integer subscript m represents the m th-order diffraction. The integer h represents the h th-harmonic grating. Diffraction occurs when the h th-harmonic grating satisfies or nearly satisfies the Bragg condition $m_h \lambda = 2(L/h) \sin\theta_o$, where m_h represents the m_h th mode (with respect to the h th-harmonic grating) excited due to the h th-harmonic grating. Exact-Bragg conditions occur when m_h is equal to m/h where h divides evenly into m. Near-Bragg conditions occur for the wavelength λ 1) when the angle of

incidence is near, but not equal to θ_o, and/or 2) when the value of m is large, and h divides nearly evenly into m, so that m/h is almost an integer. Thus, $\tilde{S}_m(z)$ in Eq. (6) represents the total amplitude, together with the propagation factor in the z direction, of the diffracted mode due to all of the gratings that satisfy or nearly satisfy the foregoing Bragg condition. At the boundary z = d, $\tilde{S}_o$ propagates at the angle θ_o, whereas $\tilde{S}_m$ propagates at an angle θ_m, which is determined by

$$\theta_m = -\sin^{-1}\left(\frac{\eta_m}{k}\right) = -\sin^{-1}\left(\sin\theta_o - \frac{m\lambda}{L}\right) \tag{7}$$

The diffracted modes due to the gratings that are far from obeying the Bragg condition are assumed to be negligibly small compared with $\tilde{S}_o$ and $\tilde{S}_m$. Therefore, the interaction between $\tilde{S}_o$ and $\tilde{S}_m$ can be characterized by the coupled-mode equations[22]

$$\frac{d\tilde{S}_o}{dz} - j\bar{\xi}_o\tilde{S}_o - j\left[\sum_h^m (C_{chm_h} + jC_{shm_h})\right]\tilde{S}_m = 0, \tag{8}$$

$$\frac{d\tilde{S}_m}{dz} - j\bar{\xi}_m\tilde{S}_m - j\left[\sum_h^m (C_{chm_h} - jC_{shm_h})\right]\tilde{S}_o = 0, \tag{9}$$

where $\bar{\xi}_o$ and $\bar{\xi}_m$ are the longitudinal wave numbers inside the medium when the gratings are absent. They are given by $\bar{\xi}_o = k(\epsilon_{ro})^{\frac{1}{2}}\cos\varphi$ and $\bar{\xi}_m = \{k^2\epsilon_{ro} - [k(\epsilon_{ro})^{\frac{1}{2}}\sin\varphi - (2m\pi/L)]^2\}^{\frac{1}{2}}$, where φ, the refraction angle in the medium, is given by $\varphi = \sin^{-1}[(\sin\theta_o)/(\epsilon_{ro})^{\frac{1}{2}}]$. The bar notation will henceforth be used to denote the quantities inside the medium when the gratings are absent. For a given value of the integer m, the subscript h may be any integer that divides evenly or nearly evenly into m, provided the corresponding h th-harmonic

grating exists. The symbol $\sum_{h}^{m}$ denotes the summation over all of these possible values of h. The coupling coefficients in Eqs. (8) and (9) are given by[17,21]

$$C_{chm_h} \cong \frac{1}{\bar{\xi}_o + \bar{\xi}_m} \left[\frac{1}{(2)^{(m_h-1)}(m_h-1)!} \right]^2 \left(\frac{\pi}{L/h} \right)^2 (q_{ch})^{m_h}, \tag{10}$$

$$C_{shm_h} \cong \frac{1}{\bar{\xi}_o + \bar{\xi}_m} \left[\frac{1}{(2)^{(m_h-1)}(m_h-1)!} \right]^2 \left(\frac{\pi}{L/h} \right)^2 (q_{sh})^{m_h}. \tag{11}$$

If the grating does not exist, $C_{chm_h} = C_{shm_h} = 0$, there is no coupling between $\bar{S}_o$ and $\bar{S}_m$ and therefore no diffraction. Under this condition, only Eq. (8) has physical significance. It represents the propagation of the fundamental mode (incident wave) inside the medium.

The solutions of Eqs. (8) and (9) are of the form

$$\tilde{S}_o(z) = A_o \exp(j\tilde{\xi}_o z) + B_o \exp(j\tilde{\xi}_m z), \tag{12}$$

$$\tilde{S}_m(z) = A_m \exp(j\tilde{\xi}_o z) + B_m \exp(j\tilde{\xi}_m z). \tag{13}$$

The wave numbers $\tilde{\xi}_o$ and $\tilde{\xi}_m$ can be found directly by substituting Eqs. (12) and (13) into Eqs. (8) and (9). They are

$$\tilde{\xi}_{o,m} = \frac{\bar{\xi}_o + \bar{\xi}_m}{2} \pm \left[\left(\frac{\bar{\xi}_o - \bar{\xi}_m}{2} \right)^2 + \left(\sum_{h}^{m} C_{chm_h} \right)^2 + \left(\sum_{h}^{m} C_{shm_h} \right)^2 \right]^{\frac{1}{2}}, \tag{14}$$

where the + sign corresponds to $\tilde{\xi}_o$ and the - sign to $\tilde{\xi}_m$. The constants A_o, B_o, A_m, and B_m are determined by the boundary conditions and

$$\left[\sum_{h}^{m} (C_{chm_h} - jC_{shm_h}) \right] A_o - (\tilde{\xi}_o - \bar{\xi}_m) A_m = 0, \tag{15}$$

$$\left[\sum_{h}^{m} (C_{chm_h} - jC_{shm_h})\right]B_o - (\tilde{\xi}_m - \bar{\xi}_m)B_m = 0, \tag{16}$$

which are obtained from Eqs. (9), (12), and (13). To specify the boundary conditions, the amplitude of the incident wave is assumed to be unity at z=0 so that, from Eq. (12),

$$\tilde{S}_o(0) = A_o + B_o = 1. \tag{17}$$

Initially, the amplitude of the diffracted wave is zero. Therefore, evaluating Eq. (13) at z = 0 gives

$$\tilde{S}_m(0) = A_m + B_m = 0. \tag{18}$$

Solving Eqs. (15), (16), (17), and (18) for A_o, B_o, A_m, and B_m gives

$$A_o = \frac{\tilde{\xi}_o - \bar{\xi}_m}{\tilde{\xi}_o - \tilde{\xi}_m}$$

$$= \frac{1}{2} \frac{(\bar{\xi}_o - \bar{\xi}_m) + \left\{(\bar{\xi}_o - \bar{\xi}_m)^2 + 4\left[\left(\sum_{h}^{m} C_{chm_h}\right)^2 + \left(\sum_{h}^{m} C_{shm_h}\right)^2\right]\right\}^{\frac{1}{2}}}{\left\{(\bar{\xi}_o - \bar{\xi}_m)^2 + 4\left[\left(\sum_{h}^{m} C_{chm_h}\right)^2 + \left(\sum_{h}^{m} C_{shm_h}\right)^2\right]\right\}^{\frac{1}{2}}}, \tag{19}$$

$$B_o = \frac{\bar{\xi}_m - \tilde{\xi}_m}{\tilde{\xi}_o - \tilde{\xi}_m}$$

$$= \frac{1}{2} \frac{(\bar{\xi}_m - \bar{\xi}_o) + \left\{(\bar{\xi}_o - \bar{\xi}_m)^2 + 4\left[\left(\sum_{h}^{m} C_{chm_h}\right)^2 + \left(\sum_{h}^{m} C_{shm_h}\right)^2\right]\right\}^{\frac{1}{2}}}{\left\{(\bar{\xi}_o - \bar{\xi}_m)^2 + 4\left[\left(\sum_{h}^{m} C_{chm_h}\right)^2 + \left(\sum_{h}^{m} C_{shm_h}\right)^2\right]\right\}^{\frac{1}{2}}}, \tag{20}$$

$$A_m = -B_m = \frac{\left(\sum_{h}^{m} C_{chm_h}\right) - j\left(\sum_{h}^{m} C_{shm_h}\right)}{\left\{(\bar{\xi}_o - \bar{\xi}_m)^2 + 4\left[\left(\sum_{h}^{m} C_{chm_h}\right)^2 + \left(\sum_{h}^{m} C_{shm_h}\right)^2\right]\right\}^{\frac{1}{2}}}. \tag{21}$$

For the exact-Bragg condition, $\bar{\xi}_m = \bar{\xi}_o$ and $\theta_m = \theta_o$. Hence, Eqs. (14), (19), (20), and (21) become

$$\tilde{\xi}_{o,m} = \bar{\xi}_o \pm [(\sum_h^m C_{chm_h})^2 + (\sum_h^m C_{shm_h})^2]^{\frac{1}{2}}, \tag{22}$$

$$A_o = 1/2 = B_o, \tag{23}$$

$$A_m = -B_m = \frac{1}{2} \frac{(\sum_h^m C_{chm_h}) - j(\sum_h^m C_{shm_h})}{[(\sum_h^m C_{chm_h})^2 + (\sum_h^m C_{shm_h})^2]^{\frac{1}{2}}}. \tag{24}$$

Thus, the transmitted and the diffracted modes are

$$\tilde{S}_o(z) = \exp(j\bar{\xi}_o z) \cos\{[(\sum_h^m C_{chm_h})^2 + (\sum_h^m C_{shm_h})^2]^{\frac{1}{2}} z\}, \tag{25}$$

$$\tilde{S}_m(z) = j2A_m \exp(j\bar{\xi}_o z) \sin\{[(\sum_h^m C_{chm_h})^2 + (\sum_h^m C_{shm_h})^2]^{\frac{1}{2}} z\}, \tag{26}$$

where C_{chm_h} and C_{shm_h} are given by Eqs. (10) and (11) with $\bar{\xi}_m = \bar{\xi}_o$, and A_m is given by Eq. (24). Eq. (26) is the general formula for the m th-diffracted mode due to any periodic grating when the incident angle of the zeroth mode satisfies the Bragg condition $m\lambda = 2L \sin\theta_o$. The diffraction efficiency for the m th order of diffraction is defined as

$$DE_m \triangleq \frac{\tilde{S}_m(d)\, \tilde{S}_m^*(d)}{\tilde{S}_o(0)\, \tilde{S}_o^*(0)}, \tag{27}$$

and thus for exact-Bragg conditions

$$DE_m = \sin^2\{[(\sum_h^m C_{chm_h})^2 + (\sum_h^m C_{shm_h})^2]^{\frac{1}{2}} d\}, \tag{28}$$

where the asterisk * denotes complex conjugate. Upon substituting Eqs. (10)

and (11), with $\bar{\xi}_m = \bar{\xi}_o$, into Eq. (28) and performing some algebraic manipulations, we find that

$$DE_m = \sin^2\left[\left(\left\{\sum_h^m \frac{1}{(2)^{m_h}}\left[\frac{1}{(m_h-1)!\ (h)^{(m_h-1)}}\right]^2 \frac{L^{2(m_h-1)}}{\lambda^{(2m_h-1)}} \frac{\pi(\epsilon_{ch})^{m_h}}{(\epsilon_{ro})^{\frac{1}{2}}\cos\varphi}\right\}^2 + \left\{\sum_h^m \frac{1}{(2)^{m_h}}\left[\frac{1}{(m_h-1)!\ (h)^{(m_h-1)}}\right]^2 \frac{L^{2(m_h-1)}}{\lambda^{(2m_h-1)}} \frac{\pi(\epsilon_{sh})^{m_h}}{(\epsilon_{ro})^{\frac{1}{2}}\cos\varphi}\right\}^2\right)^{\frac{1}{2}} d\right]. \quad (29)$$

Eq. (29) is the general expression for the diffraction efficiency at the m th-order Bragg angle for a periodic grating of arbitrary grating shape. For example, the first-, second-, and third-order diffraction efficiencies for a grating, whose dielectric constant profile can be expressed as a Fourier sine series, are

$$DE_1 = \sin^2\left[\frac{\epsilon_{s1}\pi d}{2\lambda(\epsilon_{ro})^{\frac{1}{2}}\cos\varphi}\right], \quad (30)$$

$$DE_2 = \sin^2\left\{\left[\frac{L^2(\epsilon_{s1})^2}{2\lambda^2} + \epsilon_{s2}\right]\frac{\pi d}{2\lambda(\epsilon_{ro})^{\frac{1}{2}}\cos\varphi}\right\}, \quad (31)$$

and

$$DE_3 = \sin^2\left\{\left[\frac{L^4(\epsilon_{s1})^3}{16\lambda^4} + \epsilon_{s3}\right]\frac{\pi d}{2\lambda(\epsilon_{ro})^{\frac{1}{2}}\cos\varphi}\right\}. \quad (32)$$

In Eqs. (30), (31), and (32), only the Fourier grating components ϵ_{s1}, ϵ_{s2}, and ϵ_{s3} are required to evaluate the diffraction efficiencies DE_1, DE_2, and DE_3. Table I gives these Fourier components, normalized to the amplitude of the fundamental grating, ϵ_{s1}, for gratings having sinusoidal, square-wave, triangular, and saw-tooth dielectric constant profiles. Note that the sinusoidal, square-

wave, and triangular grating shapes can each be represented by a Fourier cosine series also. In this case, the resultant diffraction efficiency expressions contain only ϵ_{c1}, ϵ_{c2}, and ϵ_{c3}. If $n_{ch} \ll n_o$ and $n_{sh} \ll n_o$, which are true in most cases[1], it can be shown that $\epsilon_{ch} = 2n_o n_{ch}$ and $\epsilon_{sh} = 2n_o n_{sh}$. Therefore, with $(\epsilon_{ro})^{\frac{1}{2}} = n_o$, Eq. (29) becomes

$$DE_m = \sin^2 \Big\{ \Big(\Big\{ \sum_h^m \Big[\frac{1}{(m_h-1)!\ (h)^{(m_h-1)}} \Big]^2 \frac{L}{\lambda}^{2(m_h-1)} \frac{\pi (n_o)^{(m_h-1)} (n_{ch})^{m_h}}{(2m_h-1)\cos\varphi} \Big\}^2 + \Big\{ \sum_h^m \Big[\frac{1}{(m_h-1)!\ (h)^{(m_h-1)}} \Big]^2 \frac{L}{\lambda}^{2(m_h-1)} \frac{\pi (n_o)^{(m_h-1)} (n_{sh})^{m_h}}{(2m_h-1)\cos\varphi} \Big\}^2 \Big)^{\frac{1}{2}} d \Big\}. \quad (33)$$

The results calculated with Eqs. (30), (31), and (32) do not agree with those calculated by use of Burckhardt's matrix method. This is because Burckhardt takes the boundary reflections into account, whereas they are not included in the foregoing derivation. Our results may be corrected to include boundary reflections by multiplying the diffraction efficiency by the transmittance factor,

$$\tau_m = \frac{(1-R)^2 [1+2R\cos(2\beta d)+R^2]}{(1-R^2)^2 + 4R^2[\cos^2(2\nu_m d)+\cos^2(2\beta d)] - 4R(1+R^2)\cos(2\nu_m d)\cos(2\beta d)}, \quad (34)$$

where $R = \sin^2(\theta_o - \varphi)/\sin^2(\theta_o+\varphi)$, $\beta = 2\pi(\epsilon_{ro})^{\frac{1}{2}}(\cos\varphi)/\lambda$, and $\nu_m = [(\sum_h^m C_{chm_h})^2 + (\sum_h^m C_{shm_h})^2]^{\frac{1}{2}}$ evaluated with $\bar{\xi}_m = \bar{\xi}_o$ for exact-Bragg conditions. This factor is the same as the transmittance factor derived by Kogelnik and given as Eq. (8) in Ref. 18, but with νd in that equation replaced by the argument of the sine function in Eq. (28) of this paper. This allows generalization to higher diffraction orders and nonsinusoidal gratings.

RESULTS AND DISCUSSION

The coupled-wave analysis in the preceding section was numerically implemented on a UNIVAC 1108 computer and calculations were performed for gratings having sinusoidal, square-wave, triangular, and saw-tooth distributions of the dielectric constant. Table II gives numerical values for the diffraction efficiencies at the first-, second-, and third-order Bragg angles for these gratings. These results represent $DE_1\ \tau_1$, $DE_2\ \tau_2$, and $DE_3\ \tau_3$ as obtained from Eqs. (30), (31), (32), and (34) with $\epsilon_{ro} = 2.3225$ (value used in Refs. 14 and 18) and $\epsilon_{s1} = 10^{-4}\epsilon_{ro}$. The fundamental spacing of these gratings is L = 3.630 μm (resulting from recording with two beams of $\lambda = 632.8$ nm at $\theta_o = \pm 5.0^o$). For comparison, the results obtained by extending Burckhardt's numerical method (matrix method) to nonsinusoidal gratings are also shown in Table II. These results were calculated by programming Burckhardt's method on a UNIVAC 1108 computer and using the UNIVAC Math Pack subroutines to solve the eigenvalue problem and the set of linear algebraic equations. Table II shows that the results of these two methods are in close agreement; the deviation between these two methods does not exceed 2.8% for diffraction efficiencies larger than 5×10^{-6}%. Diffraction efficiencies smaller than 5×10^{-6}% are less significant physically because the corresponding low-level diffracted intensities are difficult to measure. Diffraction efficiencies of less than 5×10^{-8}% have been listed as zero in Table II. In addition to the results in Table II, we have performed calculations for other grating thicknesses (15μm, 50μm, 1500μm, and 2000μm) and other fundamental grating spacings (1.222μm and 1.822μm). We found that the deviation between the coupled-wave analysis and the matrix analysis does not exceed 6.7% for any case with a diffraction efficiency larger than

5×10^{-6}%. Typically, the percentage deviation is a few tenths of one percent.

Although Burckhardt's numerical approach is rigorous, a number of mathematical problems such as truncation of the matrix and discarding of large positive eigenvalues must be overcome. A discussion of these is included in Ref. 14. In addition, another mathematical difficulty associated with the Burckhardt method, encountered in the present work, is a singularity that arises in the process of solving a set of linear algebraic equations. For pure phase gratings, Eq. (9) in Ref. 14 is real and symmetric. When the incident wave is at the Bragg angle, pairs of equal elements are introduced on the principal diagonal of the matrix in that equation. Thus, when the modulation amplitude is small, pairs of equal eigenvalues are usually induced. This results in a singularity in the matrix in Eq. (34) in Ref. 14; therefore, the equation is nonsolvable. For the parameters in the particular examples of Ref. 14, this problem does not occur because the modulation amplitude is large ($0.0035\ \varepsilon_{ro}$). However, the modulation amplitude may, in practice, be very small (of the order 10^{-4} or smaller) and the singularity problem must, therefore, be overcome. A way to avoid the singularity is by shifting the incident angle by a negligible amount away from the Bragg angle. Physically, because the shift is negligibly small (10^{-5} degrees was used here), the incident wave can still be regarded as being incident at the Bragg angle. In the present method, a closed-form expression for the diffraction efficiency is obtained, and no mathematical difficulties arise in the process of calculation. The computer time needed in the present method is only about 1/20 of that needed with the extended Burckhardt method to perform the same calculations.

From the results, we found that boundary reflections produced by the surfaces

can considerably change the diffraction efficiency. The change can be an increase or a decrease depending on whether the transmittance factor is greater or less than unity. This effect has been studied by Cohen and Gordon.[23] For the grating parameters used here, τ is typically in the range 0.70 to 1.20. In practice, the boundary reflections can be eliminated by antireflection coatings on the surfaces of the gratings. We also found that the diffraction efficiency of a given higher order is mainly contributed by the corresponding higher-order Fourier component of the grating. The difference between the diffraction efficiencies for sinusoidal and nonsinusoidal gratings (having the same average and fundamental grating amplitudes) appears only in the higher-order diffractions. The higher-order diffraction efficiencies, however, very strongly depend on the grating shape. Also, for small grating modulations, the diffraction efficiencies at any order are very dependent on grating thickness; they increase with increasing thickness. Marcuse[24] has suggested that, for small-amplitude thick nonsinusoidal phase gratings, the higher-order diffraction efficiencies might be estimated from the relative amplitudes of the spatial harmonics, consistent with the assumption of perturbation theory that only one Fourier component can satisfy the Bragg condition for a given wavelength incident wave. Our calculations show that this is true except when the amplitude of the harmonic grating ($h = m$) is very small compared to the amplitude of the fundamental and the lower-order contributing harmonic gratings. In this case, the contributions from higher-order diffractions ($h < m$) are significant. In addition, we found that the agreement between the coupled-wave method and the matrix method is better when the $h = m$ term is dominant over $h < m$ terms. Rigrod[25] has shown that for reflection gratings there is no correlation between higher-order diffraction efficiencies and the corresponding harmonics of the index profile. The present results show that

this is not true for transmission gratings.

The present method can be used to analyze the diffraction efficiency of any thick periodic grating regardless of the dielectric constant profile (grating shape). The examples analyzed here have had even or odd symmetry. However, the method does not require any symmetry to exist, but only that the grating be periodic. From the gratings analyzed, different grating shapes have shown different distributions of higher-order diffraction efficiencies. This indicates the possibility that this type of analysis might be used in reverse to determine the grating shapes of thick hologram gratings such as those recorded in ferroelectric crystals.[26] Due to nonlinearities in these materials, a sinusoidal exposure does not necessarily produce a sinusoidal change in index of refraction. Depending on which of the possible physical mechanisms is operative in a given situation (such as drift of charge carriers or diffusion of carriers) different grating shapes are generated.[27]

Further, the derivations in the preceding section have assumed that the grating medium is lossless, that the gratings are unslanted with respect to the grating boundaries (grating vector parallel to surfaces of medium), and that the incident wave is H mode polarized. If the medium is lossy, the results still apply except that the coupling coefficients are complex, and therefore the attenuation factors are implicitly contained in the expressions for the transmitted wave and the diffracted wave. The method presented here can also be straightforwardly applied to the analysis of slanted gratings and to E mode polarization of the incident wave.

CONCLUSIONS

A simple method of calculating arbitrary-order diffraction efficiencies of thick transmission gratings with arbitrary periodic grating shapes has been presented. The analysis uses a coupled-mode theory to obtain a closed-form expression for the diffraction efficiency of an arbitrary order. This method provides results with relative computational ease and results that are in close agreement with those obtained by extending Burckhardt's numerical method.

ACKNOWLEDGEMENT

The authors are indebted to Frank G. Kaspar for his helpful comments on this work.

REFERENCES

*This work was supported by the National Science Foundation under Grant No. GK-37453 and by the National Aeronautics and Space Administration under Contract No. NAS8-30246.

[1]H. Kogelnik, Bell Syst. Tech. J. 48, 2909 (1969).

[2]M. R. B. Forshaw, Opt. and Laser Technol. 6, 28 (1974).

[3]B. H. Crawford, J. Sci. Instr. 31, 333 (1954).

[4]J. N. Latta and R. C. Fairchild, J. Opt. Soc. Am. 63, 487 (1973).

[5]R. Shubert and J. H. Harris, J. Opt. Soc. Am. 61, 154 (1971).

[6]H. Kogelnik and C. V. Shank, Appl. Phys. Lett. 18, 152 (1971).

[7]I. P. Kaminow, H. P. Weber, and E. A. Chandross, Appl. Phys. Lett. 18, 497 (1971).

[8]H. Kogelnik and T. P. Sosnowski, Bell Syst. Tech. J. 49, 1602 (1970).

[9]M. L. Dakss, L. Kuhn, P. F. Heidrich, and B. A. Scott, Appl. Phys. Lett. 16, 523 (1970).

[10]J. M. Hammer, Appl. Phys. Lett. 18, 147 (1971).

[11]P. J. van Heerden, Appl. Opt. 2, 393 (1963).

[12]K. S. Pennington and L. H. Lin, Appl. Phys. Lett. 7, 56 (1965).

[13]G. W. Stroke and A. E. Labeyrie, Phys. Lett. 20, 368 (1966).

[14]C. B. Burckhardt, J. Opt. Soc. Am. 56, 1502 (1966).

[15] P. Phariseau, Proc. Indian Acad. Sci. 44A, 165 (1956).

[16] C. F. Quate, C. D. W. Wilkinson and D. K. Winslow, Proc. IEEE 53, 1604 (1965).

[17] R. S. Chu and T. Tamir, IEEE Tran. Micro. Thry. Tech. 18, 486 (1970).

[18] H. Kogelnik, J. Opt. Soc. Am. 57, 431 (1967).

[19] F. G. Kaspar, J. Opt. Soc. Am. 63, 37 (1973).

[20] T. Tamir and H. C. Wang, Can. J. Phys. 44, 2073 (1966).

[21] T. Tamir, Can. J. Phys. 44, 2461 (1966).

[22] D. A. Watkins, Topics in Electromagnetic Theory (Wiley, New York, 1958).

[23] M. G. Cohen and E. I. Gordon, Bell Syst. Tech. J. 45, 945 (1966).

[24] D. Marcuse, Light Transmission Optics (Van Nostrand Reinhold, N. Y., 1972), p. 71.

[25] W. W. Rigrod, J. Opt. Soc. Am. 64, 97 (1974) and erratum, J. Opt. Soc. Am. 64, 895 (1974).

[26] F. S. Chen, J. T. LaMacchia and D. B. Fraser, Appl. Phys. Lett. 13, 223 (1968).

[27] J. J. Amodei, RCA Rev. 32, 185 (1971).

FIGURE CAPTION

Figure 1. Geometry of a thick grating with unslanted fringes. The spatial modulation of ε is indicated by the line pattern.

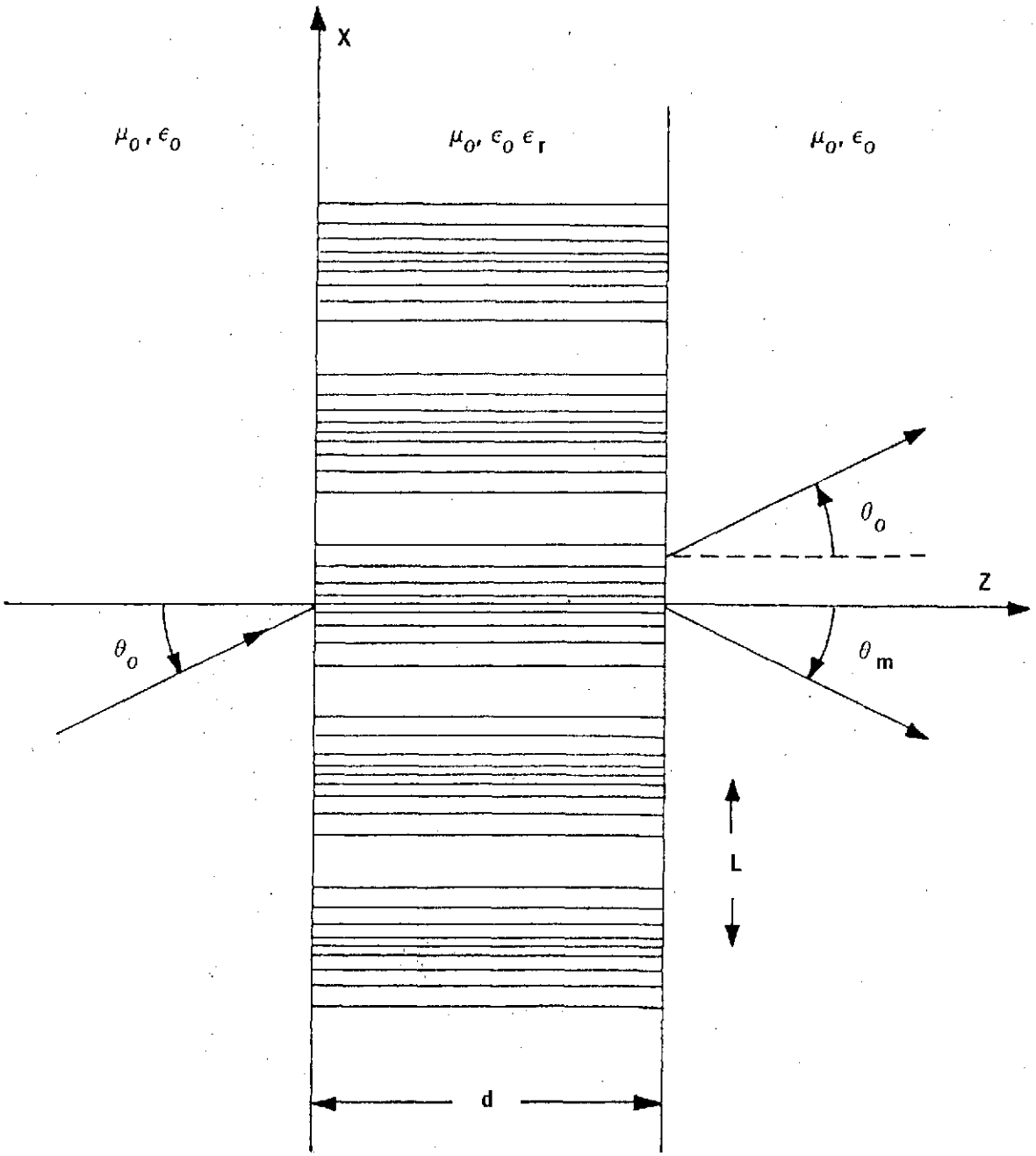
X
μ_0, ϵ_0
$\mu_0, \epsilon_0 \epsilon_r$
μ_0, ϵ_0
θ_o
Z
θ_o
θ_m
L
d

Fig. 1

TABLE I. First three Fourier components for various relative dielectric constant profiles (grating shapes). Components are normalized to the amplitude of the fundamental grating, ϵ_{s1}.

Grating Component	Sinusoidal grating	Square-wave grating	Triangular grating	Saw-tooth grating
$\epsilon_{s1}/\epsilon_{s1}$	1	1	1	1
$\epsilon_{s2}/\epsilon_{s1}$	0	0	0	-1/2
$\epsilon_{s3}/\epsilon_{s1}$	0	1/3	-1/9	1/3

TABLE II. Comparison of diffraction efficiency in percent at the first-, second-, and third-order Bragg angles for transmission gratings with boundary reflections and with the same average and fundamental Fourier grating components. The grating parameters are $\epsilon_{ro} = 2.3225$ (value used in Refs. 14 and 18), $\epsilon_{s1} = 10^{-4}\epsilon_{ro}$, $L = 3.6303\,\mu m$, and the wavelength $\lambda = 0.6328\,\mu m$. Diffraction efficiencies of less than $5 \times 10^{-8}\%$ are listed as 0.00(-5).

Grating thickness (microns)	Diffraction order	Diffraction Efficiency (in % with power of ten in parentheses)							
		Sinusoidal grating		Square-wave grating		Triangular grating		Saw-tooth grating	
		Coupled-wave	Matrix	Coupled-wave	Matrix	Coupled-wave	Matrix	Coupled-wave	Matrix
10	1	1.64(-3)	1.64(-3)	1.64(-3)	1.64(-3)	1.64(-3)	1.64(-3)	1.64(-3)	1.64(-3)
	2	0.00(-5)	0.00(-5)	0.00(-5)	0.00(-5)	0.00(-5)	0.00(-5)	3.81(-4)	3.87(-4)
	3	0.00(-5)	0.00(-5)	1.14(-4)	1.14(-4)	1.26(-5)	1.25(-5)	1.14(-4)	1.13(-4)
100	1	1.57(-1)	1.57(-1)	1.57(-1)	1.57(-1)	1.57(-1)	1.57(-1)	1.57(-1)	1.57(-1)
	2	0.15(-5)	0.13(-5)	0.15(-5)	0.14(-5)	0.15(-5)	0.13(-5)	2.49(-2)	2.56(-2)
	3	0.00(-5)	0.00(-5)	1.12(-2)	1.12(-2)	1.25(-3)	1.23(-3)	1.12(-2)	1.12(-2)
1000	1	1.21(+1)	1.21(+1)	1.21(+1)	1.21(+1)	1.21(+1)	1.21(+1)	1.21(+1)	1.21(+1)
	2	2.53(-4)	2.46(-4)	2.53(-4)	2.46(-4)	2.53(-4)	2.46(-4)	4.16(+0)	4.26(+0)
	3	0.00(-5)	0.00(-5)	1.64(+0)	1.64(+0)	1.83(-1)	1.84(-1)	1.64(+0)	1.66(+0)

IX. SYSTEMS CONSIDERATIONS

A three-dimensional lithium niobate recording and storage system is shown schematically in Fig. 8. The systems aspects of such an optical recording scheme were thoroughly reviewed in this study. One of the results of this review was the publication of a state-of-the-art review [6]. This article is reproduced in this report and is a self-contained review. Another result of this review was a change in our experimental reading system. An angular accessing system was developed and it is illustrated in Fig. 9. This system allows accurate and simple angular beam positioning without the need to rotate the crystal.

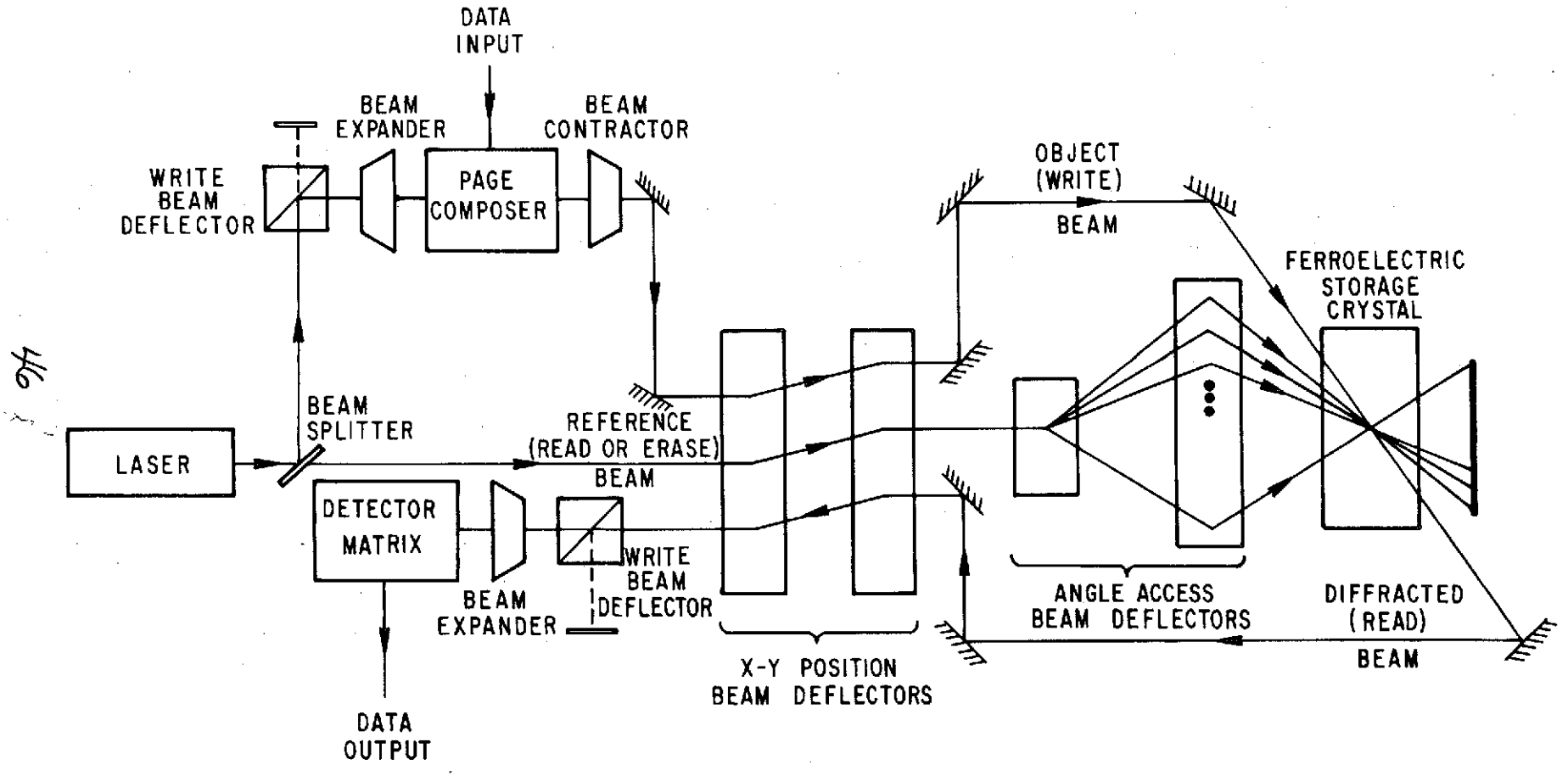

FIGURE 8. SCHEMATIC OF A READ-WRITE-ERASE OPTICAL HOLOGRAPHIC COMPUTER MEMORY.

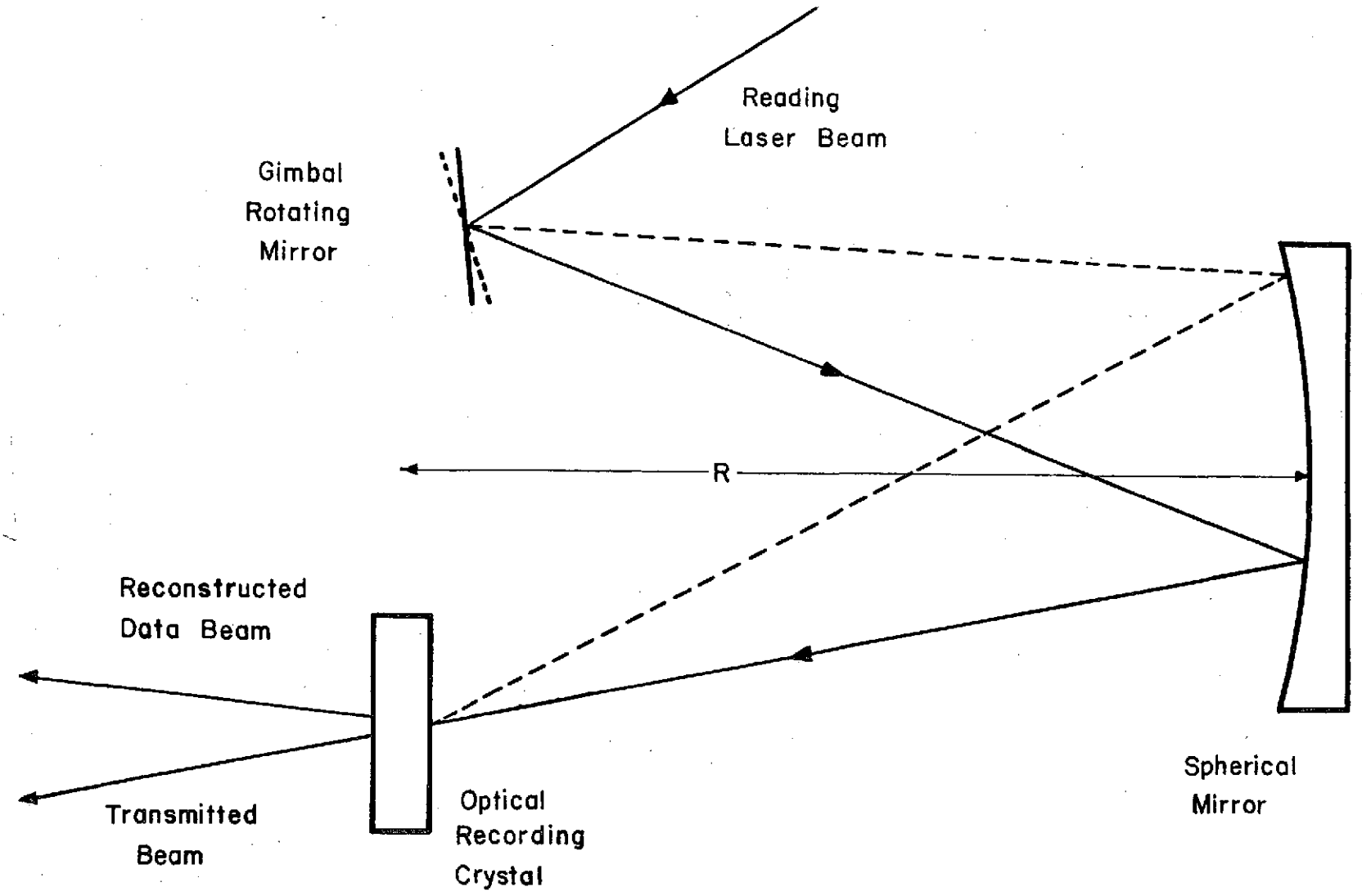

FIGURE 9. ANGULAR ACCESS SCANNER FOR READING MULTIPLE HOLOGRAMS STORED AT A SINGLE LOCATION.

OPTICAL MEMORIES

FILLING THE STORAGE GAP

BY THOMAS K GAYLORD

PAPER INTENTIONALLY OMITTED

REFERENCES

[1] H. Kogelnik, "Coupled wave theory for thick hologram gratings," Bell System Tech. J., Vol. 48, No. 4, pp. 2902-2947, November 1969.

[2] T. K. Gaylord and F. K. Tittel, "Angular selectivity of lithium niobate holograms," J. Appl. Phys., Vol. 44, No. 9, September 1973.

[3] S. F. Su and T. K. Gaylord, "Calculation of arbitrary-order diffraction efficiencies of thick gratings with arbitrary grating shape," J. Optical Soc. of Am. (to be published).

[4] H. Kogelnik, "Bragg diffraction in hologram gratings with multiple internal reflections," J. Optical Soc. of Am., Vol. 57, pp. 431-433, March 1967.

[5] M. G. Cohen and E. I. Gordon, "Acoustic scattering of light in Fabry-Perot resonator," Bell System Tech. J., Vol. 45, pp. 945-966, July-August 1966.

[6] T. K. Gaylord, "Optical memories," Optical Spectra, Vol. 8, No. 6, pp. 29-34, June 1974.

[7] F. S. Chen, J. T. LaMacchia, and D. B. Fraser, "Holographic storage in lithium niobate," Appl. Phys. Letters, Vol. 13, pp. 223-225, October 1, 1968.

[8] P. Shah, T. A. Rabson, F. K. Tittel, and T. K. Gaylord, "Volume holographic recording and storage in Fe-doped $LiNbO_3$ using optical pulses," Appl. Phys. Letters, Vol. 24, No. 3, pp. 130-131, February 1974.

[9] D. von der Linde, A. M. Glass, and K. F. Rogers, "Multiphoton photorefractive processes for optical storage in $LiNbO_3$," Appl. Phys. Letters, Vol. 25, No. 3, pp. 155-157, August 1, 1974.

[10] W. Phillips, J. J. Amodei, and D. L. Staebler, "Optical and holographic storage properties of transition metal doped lithium niobate," RCA Review, Vol. 33, No. 1, pp. 94-109, March 1972.

[11] R. Magnusson and T. K. Gaylord, "Laser scattering induced holograms in lithium niobate," Appl. Optics, Vol. 13, No. 7, pp. 1545-1548, July 1974.

[12] J. M. Moran and I. P. Kaminow, "Properties of holographic gratings photo-induced in polymethyl methacrylate," Applied Optics, Vol. 12, pp. 1964-1970, August 1973.

[13] D. L. Staebler, J. J. Amodei, and W. Phillips, "Multiple storage of thick phase holograms in $LiNbO_3$," Digest of Technical Papers, 1972 International Quantum Electronics Conference, p. 93, May 8-17, 1972.

[14] P. J. van Heerden, "Theory of optical information storage in solids," Appl. Optics, Vol. 2, No. 4, pp. 393-400, April 1963.

[15] L. d'Auria, J. P. Huignard, C. Siezak, and E. Spitz, "Experimental holographic read-write memory using 3-D storage," Applied Optics, Vol. 13, No. 4, pp. 808-818, April 1974.

[16] J. J. Amodei and D. L. Staebler, "Holographic recording in lithium niobate," RCA Review, Vol. 33, No. 1, pp. 71-93, March 1972.

[17] D. L. Staebler and W. Phillips, "Fe-doped $LiNbO_3$ for read-write applications," Appl. Optics, Vol. 13, No. 4, pp. 788-794, April 1974.

[18] C. B. Burckhardt, "Diffraction of a plane wave at a sinusoidally stratified dielectric grating," J. Optical Soc. Am., Vol. 56, pp. 1502-1509, November 1966.